

Precision Method for Hyperfine-Structure Studies in Low-Abundance Isotopes: The Quadrupole Moment of ^{43}Ca

P. Grundevik, M. Gustavsson, I. Lindgren, G. Olsson, L. Robertsson,
A. Rosén, and S. Svanberg

Department of Physics, Chalmers University of Technology, S-412 96 Göteborg, Sweden

(Received 12 April 1979)

Precision hyperfine-structure measurements in the $4s4p\ ^3P_2$ metastable state of ^{43}Ca were performed using the atomic-beam magnetic-resonance method combined with a single-mode dye laser for the detection. For the first time the electric quadrupole moment of the particularly interesting ^{43}Ca nucleus was accurately determined: $Q(^{43}\text{Ca}) = -0.065$ (20) b. In addition, isotope shifts and hyperfine structure in the transition $4s4p\ ^3P_2 \leftrightarrow 4s5s\ ^3S_1$ were obtained using high-resolution laser spectroscopy.

For many reasons information on the isotope shifts and hyperfine interaction for calcium isotopes is of great interest. The nuclides ^{40}Ca and ^{48}Ca are both doubly magic and isotope shift studies in the series of Ca isotopes yield information on the effects associated with the addition of neutrons in the $f_{7/2}$ shell.¹ As the only stable isotope with nonzero nuclear spin, ^{43}Ca has a static spectroscopic quadrupole moment, and a determination of this quantity yields information on the nuclear deformation. Calcium is also an element of great biological interest and in NMR studies involving this element, ^{43}Ca is the only useful isotope. Knowledge of the static quadrupole moment is necessary in order to understand different relaxation processes.² Whereas spectroscopic studies of ^{43}Ca are highly motivated, such investigations meet with considerable experimental difficulties. The isotope has a very low natural abundance (0.145%). Studies using enriched samples in sealed-off cells are hampered by the extreme chemical reactivity of calcium with common cell materials. A determination of the static moments cannot be performed in the ground state because of the electronic symmetry of this state (1S_0), and thus a suitable excited state must be chosen. Level-crossing experiments in the short-lived $4s4p\ ^1P_1$ state were performed by Kluge and co-workers^{3,4} using enriched ^{43}Ca samples in specially adapted cells. The unfavorable relation between hyperfine splittings and natural radiation width of this state prevented any decisive conclusion concerning the quadrupole moment. Recently, Neumann and co-workers^{5,6} have applied high-resolution intracavity spectroscopy for studying the very weak intercombination line $6573\ \text{\AA}$ ($4s^2\ ^1S_0 \leftrightarrow 4s4p\ ^3P_1$). These measurements have recently been revised.⁷ However, no accurate value of the quadrupole moment has yet been obtained.

In the present paper we report on precision

measurements of the hyperfine interaction in the metastable $4s4p\ ^3P_2$ state of ^{43}Ca . The atomic-beam magnetic-resonance (ABMR) technique with laser detection was used.^{8,9} For enhancing the ^{43}Ca signals a single-mode dye laser acting selectively on this isotope was used. From the measurement a useful value for the quadrupole moment was obtained for the first time. In addition, the isotope shifts in the $6162\text{-}\text{\AA}$ ($4s4p\ ^3P_2 \leftrightarrow 4s5s\ ^3S_1$) line and the magnetic dipole coupling constant for the 3S_1 state were determined in high-resolution laser-spectroscopy experiments on a collimated atomic beam.

In our experiments, two separate atomic-beam setups were used in connection with a narrow-band single-mode dye-laser spectrometer. The experimental arrangement is shown in Fig. 1. In the lower part of the figure the ABMR apparatus is shown. This equipment was used in the radio-frequency experiments and will be discussed below. In the right-hand part of the figure the collimated-atomic-beam apparatus for high-resolution optical spectroscopy studies is shown. The laser system consists of a Coherent Radiation model 599 single-mode dye laser, pumped by a 3000-K Kr^+ laser. For monitoring the single-mode sweep, two confocal spectrum analyzers with free spectral ranges (FSR) of 1.5 and 7.5 GHz, respectively, were used. An absolute determination of the laser frequency was obtained with a digital wave meter.¹⁰ An accurate frequency scale is provided with a spherical Fabry-Perot interferometer with a FSR of 50 MHz.

Atoms in metastable states were produced by means of a plasma discharge in an oven of a type described in an earlier paper.⁹ The light from the single-mode laser is irradiated at right angles to the collimated atomic beam. Fluorescent light released after the excitation is detected in a direction perpendicular to the atomic beam as well as to the laser beam.

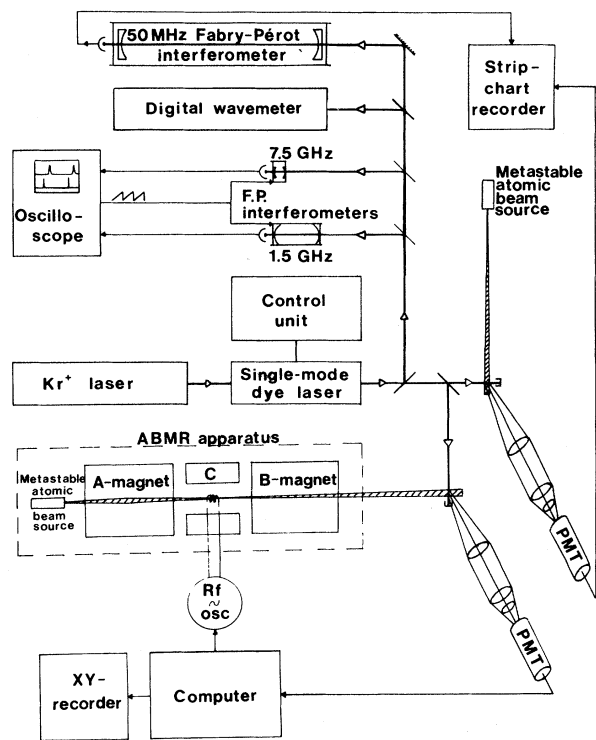


FIG. 1. Schematic diagram of the experimental setup.

An atomic energy-level diagram of the low-lying states of calcium is displayed in the left-hand side of Fig. 2. The diagram includes the transition used by Kluge and co-workers,^{3,4} and zu Putlitz and co-workers,⁵⁻⁷ as well as the transi-

tion used in the present work. This line connects the metastable $4s4p\ ^3P_2$ state with the short-lived $4s5s\ ^3S_1$ state. By studying the hyperfine structure of this line, information on the magnetic dipole [$A(^3P_2)$] and the electric quadrupole interaction constant [$B(^3P_2)$] for the 3P_2 state and the dipole interaction constant [$A(^3S_1)$] for the 3S_1 state was obtained. We performed these measurements in the collimated-atomic-beam apparatus described above. A recording obtained in a laser scan of this line is shown in Fig. 2 with the 50-MHz Fabry-Pérot fringes in the lower part of the figure. The spectrum is dominated by the strong signal from the ^{40}Ca isotope (96.97%) which in this recording has been attenuated by a factor of 10^3 . All the weak components outside the attenuated part of the curve are due to hyperfine transitions in ^{43}Ca . In the right-hand part of the figure the hyperfine energy-level diagram corresponding to the ^{43}Ca components is given. The individual components are designated with the appropriate F quantum numbers. From about 25 recordings of the type shown in Fig. 2 we deduced the hyperfine coupling constants for the 3P_2 and 3S_1 states. We obtained for the lower state $A(^3P_2) = -171.9(7)$ MHz, $B(^3P_2) = -5(5)$ MHz, and for the upper state $A(^3S_1) = -463.3(1.0)$ MHz. From the center of gravity of all the hyperfine components the isotope shift (IS) of ^{43}Ca relative to the dominating ^{40}Ca was obtained: $\Delta\nu_{\text{obs}}(43,40) = -38.2(2.0)$ MHz. It is not possible to deduce the IS between the even-even isotopes except for ^{48}Ca

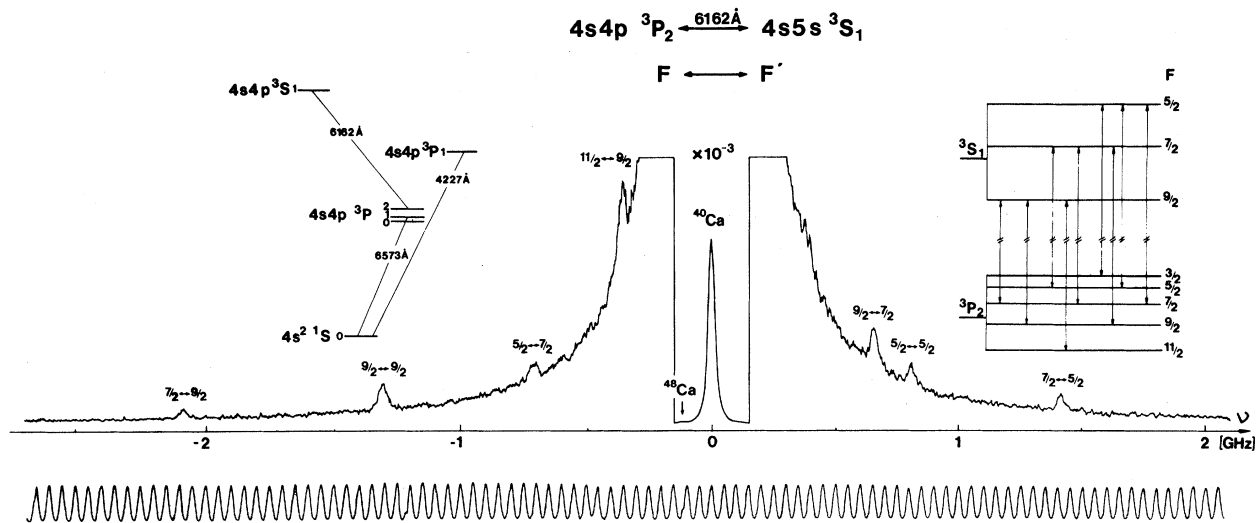


FIG. 2. High-resolution fluorescence spectrum of the 6162-Å Ca line, obtained in a single-mode laser sweep of a duration of about 4 min. In the figure a scheme of the low-lying states of Ca is included as well as a diagram of the relevant hyperfine transitions for ^{43}Ca .

(0.185%) relative to ^{40}Ca . The small ^{48}Ca component can be seen close to the center peak in the attenuated recording. From suitably amplified curves the IS was found to be $\Delta\nu_{\text{obs}}(48, 40) = -116(4)$ MHz. The normal mass shifts for this Ca line are $\Delta\nu_{\text{nms}}(43, 40) = 462.4$ MHz and $\Delta\nu_{\text{nms}}(48, 40) = 1104.6$ MHz, respectively. Thus the specific mass and volume effects give rise to the shifts $\Delta\nu(43, 40) = -500.6(2.0)$ MHz and $\Delta\nu(48, 40) = -1221(5)$ MHz. Therefore, these effects slightly overcompensate the normal mass shift.

The accuracy of the electric quadrupole interaction constant obtained for the 3P_2 state in this experiment is not sufficiently good for an evaluation of the nuclear quadrupole moment. In order to improve the accuracy, rf-resonance experiments were performed.

The atomic-beam magnetic-resonance method is suitable for studies of ground and metastable atomic states. This method is particularly powerful when combined with laser detection.^{8,9} As compared with conventional techniques, this type of detection has the advantage of being state selective, which means that the signal and the observed background emanate only from the chosen state. So far, we have used this technique with a cw dye laser in multimode operation or with a pulsed dye laser. By employment of a single-mode laser, the sensitivity and signal-to-noise ratio in the measurements is greatly improved, and in addition the detector is in most cases isotope selective. In the present experiment these features were necessary in order to get detectable signals from ^{43}Ca . In the ABMR apparatus the atoms in the metastable 3P_2 state are polarized in the inhomogeneous magnetic field of the A magnet. When radio-frequency transitions are induced between two different F levels, in the homogeneous C-field region, a depolarization of the atomic beam occurs. As a result, atoms in one of the F levels can pass the analyzing B magnet. By tuning of the single-mode laser to an optical transition from this F level to a certain hyperfine level in a higher electronic state (in our case $4s5s\ ^3S_1$), the rf transitions can be detected by the released fluorescence light following the excitation. Such suitable optical transitions can be found among the recorded ^{43}Ca components in Fig. 2. In Fig. 3, a recording of rf transitions in the $4s4p\ ^3P_2$ state is shown. For detecting these resonances the single-mode laser was tuned to the $F = \frac{9}{2} \leftrightarrow F' = \frac{7}{2}$ optical transition shown in Fig. 2. In order to ensure a correct laser tuning, this transition

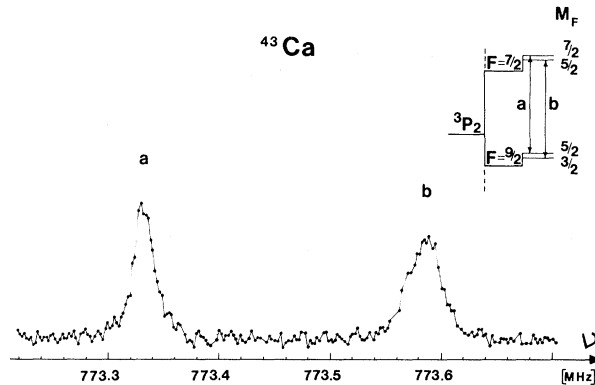


FIG. 3. Radio-frequency transitions between the $F = \frac{9}{2} \leftrightarrow F = \frac{7}{2}$ levels of the $4s4p\ ^3P_2$ state, measured in an external magnetic field of 1.075 G. The signals were recorded with the single-mode laser tuned to the $F = \frac{9}{2} \leftrightarrow F' = \frac{7}{2}$ optical transition (the third component from the right in Fig. 2). The curve was obtained by averaging repetitive radio-frequency sweeps during a total measuring time of about 15 min.

was simultaneously monitored in the collimated-beam setup. We have also measured the other observable hyperfine intervals of the 3P_2 state by tuning the rf oscillator to the proper rf frequency and the single-mode laser to the appropriate optical component. The rf transitions were driven in a low external magnetic field and the A and B factors were determined in a least-squares fit of the observed rf resonances by the hyperfine Hamiltonian. Recorded curves from fourteen different transitions covering three hyperfine intervals have been used in this procedure. We obtained

$$A(^3P_2) = -171.962(2) \text{ MHz},$$

$$B(^3P_2) = -5.436(8) \text{ MHz}.$$

For the evaluation of the quadrupole moment (Q) an *ab initio* value of the radial quadrupole parameter $\langle r^{-3} \rangle$ has been calculated using the Hartree-Fock method with the result $\langle r^{-3} \rangle_{\text{HF}} = 0.637$ a.u. This yields a quadrupole moment $Q_{\text{HF}} = -0.091$ b. This is a first-order result and it does not include polarization and correlation effects. In an analysis of the analogous $3s3p$ configuration in Mg, using the multiconfigurational Hartree-Fock method, Bauche, Couarraze, and Labarthe¹¹ estimated the higher-order effects to reduce the quadrupole moment by an amount of 40% compared to the HF value. Assuming that the situation is similar for Ca, we can estimate a corrected quadrupole moment to be $Q_{\text{HF corr}}$

= -0.054 b. More detailed calculations of polarization and correlation effects using techniques developed at our laboratory are now in progress. At present we give the following estimation of the quadrupole moment of ^{43}Ca :

$$Q(^{43}\text{Ca}) = -0.065(20) \text{ b},$$

where the limits of error are believed to bracket the unknown polarization and correlation effects.

The authors gratefully acknowledge stimulating discussions with Professor S. Forsén. Financial support from the Swedish Natural Science Research Council is gratefully recognized.

¹H.-W. Brandt, K. Heilig, H. Knöckel, and A. Steudel, *Z. Physik* **288A**, 241 (1978).

²B. Lindman and S. Forsén, in *NMR and Periodic Table*, edited by R. K. Harris and B. E. Mann (Academic, London, 1978).

³H. J. Kluge, E.-W. Otten, and G. Zimmermann, *J. Phys. (Paris), Colloq.* **30**, C-1 (1969).

⁴H. J. Kluge and H. Sauter, *Z. Phys.* **270**, 295 (1974).

⁵R. Neumann, F. Träger, J. Kowalski, and G. zu Putlitz, *Z. Phys.* **279A**, 249 (1976).

⁶F. Träger, R. Neumann, J. Kowalski, and G. zu Putlitz, *Appl. Phys.* **12**, 19 (1977).

⁷U. Klingbeil, J. Kowalski, F. Träger, H.-B. Wiegemann, and G. zu Putlitz, *Z. Phys.* **290A**, 143 (1979).

⁸M. Gustavsson, I. Lindgren, G. Olsson, A. Rosén, and S. Svanberg, *Phys. Lett.* **62A**, 250 (1977).

⁹M. Gustavsson, G. Olsson, and A. Rosén, to be published.

¹⁰F. V. Kowalski, R. T. Hawkins, and A. L. Schawlow, *J. Opt. Soc. Am.* **66**, 965 (1976).

¹¹J. Bauche, G. Couarraze, and J.-J. Labarthe, *Z. Phys.* **270**, 311 (1974).

Structure of a Shock-Wave Front in a Liquid

William G. Hoover

Department of Applied Science, University of California at Davis, Livermore, California 94550, and Lawrence Livermore Laboratory, Livermore, California 94550

(Received 4 April 1979)

Solutions of the Navier-Stokes equations for strong shock waves in a dense fluid agree well with recent atomistic simulations using nonequilibrium molecular dynamics.

In the last few years nonequilibrium molecular dynamics has been applied to the simulation of transport processes in dense fluids, where transport is dominated by interparticle forces. A significant advance in nonequilibrium molecular dynamics has just been published by Klimenko and Dremin.¹ Their novel simulations now make it possible for us to assess the usefulness of the Navier-Stokes description of strong shock waves in liquid argon. These two cases correspond to shock waves traveling at 1.8 and 2.6 km/sec. (The velocity estimate of 2.0 km/sec quoted in Ref. 1 for the weaker shock is inconsistent with the profiles published in that paper.) They used the Lennard-Jones potential

$$\varphi(r) = 4\epsilon[(\sigma/r)^{12} - (\sigma/r)^6] \quad (1)$$

with $\epsilon/k = 120 \text{ K}$ and $\sigma = 0.3405 \text{ nm}$. For both calculations the initial molar volume was 36 cm^3 and the temperature 131 K . The resulting data are of great interest because they represent the first detailed simulations of a realistic dense shocked

fluid, far from equilibrium, in which the equations of motion are solved without approximation. Previous work on shock waves has been primarily devoted to the ideal-gas case²⁻⁴ although Niki and Ono have studied an imperfect gas of hard spheres at densities up to about one-third the freezing density.⁵ Tsai⁶ and Holian and Straub⁶ have also carried out dense-fluid shock simulations. Holian and Straub have obtained preliminary results very similar to those of Ref. 1.

A hydrodynamic understanding of the atomistic shock structure requires a complete description of the constitutive behavior of the Lennard-Jones fluid. This information is now available. Ree⁷ has developed analytic expressions for the pressure and energy as functions of volume and temperature. Although similar to the Levesque-Verlet⁸ equation of state, Ree's is specifically designed to handle the high-temperature, high-density region in which equations based on the collision-diameter approach fail. Transport coefficients for the Lennard-Jones fluid are available